Performance Evaluation of Joint Passive Time Reversal and Adaptive Decision Feedback Equalizer in Shallow Water Environment

Yuning Widiarti[1,2], Wirawan[1], and Suwadi[1]
[1] Department of Electrical Engineering, Faculty of Electrical Engineering, Institut Teknologi Sepuluh Nopember, Surabaya 60111, Indonesia
[2] Shipbuilding Institute of Polytechnic Surabaya, Surabaya 60111, Indonesia
Email: yuning.widiarti@ppns.ac.id; wirawan@ee.its.ac.id; suwadi@ee.its.ac.id

Abstract —Underwater wireless communication is growing rapidly along with human needs for applications such as defense, state security, underwater control, and monitoring system. The underwater acoustic channel has many challenges such as selectivity time-space, frequency dependent noise, Doppler shift, and intersymbol interference on transmission. Time Reversal is an effective method for dealing with inter-symbol interference. In TR a signal is precoded in such a way that it focuses both in time and in space at a particular receiver. This paper evaluates the performance of joint Passive Time Reversal and Adaptive Decision Feedback Equalizer (PTR-ADFE) technique in shallow water environment. Geometry-based channel model and environmental parameters are used. In addition, the modification of the LMS algorithm at Decision Feedback Equalizer is done to improve the performance of the PTR-ADFE communication system. The simulation results show that the Bit-Error-Rate (BER) of PTR-ADFE increases significantly when compared to the BER value of equalization technique.

Index Terms—PTR communication, geometry-based channel model, shallow water environment, modified LMS, Adaptive DFE (ADFE), inter-symbol interference (ISI).

I. Introduction

In the last ten years, the Underwater Acoustic Communication (UAC) system has received much attention from most researchers. Underwater acoustic sensor networks are widely studied for having the potential applications in marine fields, such as marine exploration, underwater robots, offshore oil industry exploration, pollution monitoring, and many other examples of applications. However, the underwater channel has its own challenges, such as bandwidth limitation, high dispersive, and time-varying multipath. The presence of extended multipath has led to ISI, which results in severe distortions of the transmitted signals. ISI causes serious damage to communication signals and also difficulties in the demodulation process [1]. Thus, the communication performance can be degraded significantly because of ISI [1]-[3].

Currently, time reversal (TR) has been widely applied to several studies in the field of UAC with a relatively simple approach and has a low level of computational complexity [4]-[6]. Temporal focusing of TR property can minimize ISI, while its spatial focusing can reduce the channel fading effect and improve the Signal-to-Noise Ratio (SNR). The concepts and experiments of Active Time Reversal (ATR) communication have been shown in [1], [6], [7], and [9]. Meanwhile, the research results on Passive Time Reversal (PTR) have been discussed in [4], [9]-[11]. To reduce the complexity of a receiving array, PTR technique requires only one-way communication. In PTR, spatial diversity is obtained by sampling the sound field with multiple receivers. TR Array (TRA) is applied to implement the TR concept in PTR [12]. The array only needs to receive signals and does not need to transmit, and then each element of the array captures all signals which are transmitted by the source. The signal processing step involves cross correlating the probe receptions and data streams at an array element. This cross correlation is done in parallel at each array element and the results are summed across the array to achieve the final communication signals, which are ready for demodulation.

Although the focusing property of TR can overcome ISI, the resulting side lobes cannot be simply removed. The residual ISI can distort the transmitted information due to which one of the symbols overlaps with the subsequent symbols. Therefore, an equalizer is needed to eliminate the ISI. Over the last ten years, a number of studies have focused on the equalizer design to overcome ISI and compensate for channel variations [13], [14]. This equalization technique requires complex computation, algorithm stability, and channel parameter selection [15]. Moreover, to improve the performance of the communication system, the single channel receiver is developed into a multichannel receiver system. However, the multichannel system requires the equalization technique with high computational complexity [13], [16]. Reduction of multipath which is obtained by TR has its own challenges in the presence of a time-varying channel environment, so the perfect channel estimation is difficult to be obtained. Recently, PTR is combined with phase lock loops (PLL) to overcome time-varying underwater acoustic channel problems.

Manuscript received March 1, 2019; revised September 29, 2019.
doi:10.12720/jcm.14.11.1059-1066

Each of the TR or DFE techniques has the ability to overcome ISI and time-varying channel characteristic. Therefore, in this paper the author presents a combination of PTR and Adaptive DFE and evaluates its performance in shallow water environment. Adaptive DFE is applied after PTR processing for removal of residual ISI. The filters used here are adaptive filters where the coefficients were updated with Least Mean Square (LMS) algorithm. The LMS algorithm is convenient due to its computational simplicity. However, it has very low convergence speed. For this reason, the information frame needs longer training of bits to ensure that the iteration can reach a steady state of convergence during training mode [17]. However, it will require more bandwidth and reduce communication effectiveness. In this paper, the existing algorithm is modified to get a faster convergence and a better mean square error (MSE). This is done by implementing some constraints in the filter coefficients updating criteria. The underwater acoustic channel used in this paper is a geometry-based model. This model is simple and effective for analyzing the performance of the communication system used by considering the environmental parameters such as wind speed and sound speed in UAC. From the description above, the contributions offered in this paper are as follows:

1. Geometry-based model to represent underwater acoustic channels on the real towing tank;
2. Performance analysis of PTR communications system combined with Adaptive DFE (PTR-ADFE) on the multipath and distance between source and receiver that varies in a shallow water environment;
3. Performance analysis of Adaptive DFE with the modification of the existing LMS algorithm.

This paper is structured as follows: Section 2 is a brief review of Underwater Acoustic Communication Model, Section 3 explains Joint Passive Time Reversal and Adaptive DFE. Section 4 discusses and analyzes the PTR-ADFE simulation, and the last section is section 5 which is the conclusion of this paper.

II. Underwater Acoustic Communication (UAC) Model

A. Sound Speed

The variation of the sound speed (c) in the ocean is relatively small. Normally, c is assumed to be at 1450 to 1540 m/s. However, small variations of c have an impact on sound propagation in UAC. The sound speed can be measured directly or calculated using an empirical formula by knowing the value of temperature (T), salinity (S), and hydrostatic pressure (P). The accuracy of the most comprehensive empirical formula is comparable to that of modern velocimeter measurements. However, formulas that provide high accuracy have high complexity. A simple equation, although it has a low level of accuracy is written in the following equation:

$$c = 1450 + 4.21T - 0.0037T^2 + 1.14(S-35) + 0.175P \quad (1)$$

where c is the corresponding sound speed in m/s, T denotes the temperature (°C), S stands for salinity (%), and P denotes pressure (atm), and those environmental factors are slow time-varying during the communication. The sound speed is usually considered as a constant, which is 1500 m/s.

B. Geometry-based UAC Model

Acoustic waves are reflected on the sea surface and the surface of the sea bottom in the UAC and also reflections with obstructive objects. By assuming that the underwater acoustic sound speed is constant (c) and the water depth (h) is in uniform, the geometry channel can be represented as in Fig. 1. The notations in the figure can be explained as follows: Z_t denotes the transmitter height from the bottom; Z_r is the receiver height from the bottom; L is the distance between the transmitter and receiver; D stands for the direct path between transmitter and receiver; SS is the representation of the reflection from sea surface and sea surface; SB is a representation of the reflection from the sea surface and sea bottom; BS is a representation of the reflection from sea bottom and sea surface; BB is a representation of the reflection from the sea bottom and sea bottom; and x is a notional order for the multipath.

$$L/h >> 2x+1 \quad (2)$$

Referring to Fig. 1, each path length can be calculated using equation (3):

$$\sqrt{L^2 + A^2} \quad (3)$$

where:

$$A = Z_r - Z_t; k = -1 \, for \, D$$
$$A = 2xh - Z_t - Z_r; k = 1 \, for SS_x$$
$$A = 2xh + Z_t - Z_r; k = 1 \, for BS_x$$
$$A = 2(x-1)h + Z_t + Z_r; k = -1 \, for BB_x \quad (4)$$

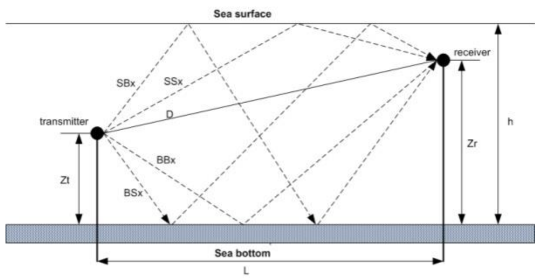

Fig. 1. The multipath channel model for underwater acoustic communication

By using binomial expansion, equation (3) can be developed into equation (5) as follows:

$$D = \sqrt{L^2 + (Z_r - Z_t)^2}$$

$$\cong \left[L + \frac{1}{2L}\left(Z_r - Z_t\right)^2 \right] \tag{5}$$

The geometry-based channel model used refers to the real condition of a towing tank that has a length of 200 m, a width of 12 m, and a depth of 6 m. The transmitted signals propagate to the receiver via direct path and multipath. To calculate the length of the direct path and the multipath, a binomial expansion is used [18]. Based on the conditions of the real towing tank, then it belongs to the shallow water, in accordance with equation (2). In the same way, for the path length of SS_x we get:

$$SS_x = \sqrt{L^2 + \left[2xh - \left(Z_t + Z_r\right)\right]^2}$$

$$\cong [L + \frac{1}{2L}\left(2xh - \left(Z_t + Z_r\right)\right)^2 \tag{6}$$

For the SB_x path, BS_x and BB_x they can be calculated by means of equations (5) and (6). While the time difference coming between SS_x and D can be calculated by equation (7) as follows:

$$\tau_{SSx} = t_{SSx} - t_D = \frac{SS_x - D}{c}$$

$$\cong \frac{2}{Lc}\left[x^2h^2 - xh\left(Z_t + Z_r\right) + Z_t Z_r \right] \tag{7}$$

where t_{ssx} stands for the arrival time of the signal from the x^{th} SS and t_D is the arrival time of direct path signal. For the time difference between SB_x, BS_x, and BB_x in the same way as in (7), we find the equations (8), (9), and (10).

$$\tau_{SBx} = t_{SBx} - t_D \cong \frac{2}{Lc}\left[x^2h^2 + xh\left(Z_r - Z_t\right) \right] \tag{8}$$

$$\tau_{BSx} = t_{BSx} - t_D \cong \frac{2}{Lc}\left[x^2h^2 + xh\left(Z_t - Z_r\right) \right] \tag{9}$$

$$\tau_{BBx} = t_{BBx} - t_D$$

$$\cong \frac{2}{Lc}\left[\left(x-1\right)^2 h^2 + \left(x-1\right)h\left(Z_t + Z_r\right) + Z_t Z_r \right] \tag{10}$$

The coefficient of surface reflection (r_s) or the bottom reflection coefficient (r_b) is used to determine the decrease in acoustic pressure at each reflection.

$$\left|\tilde{r}_s\right| = \sqrt{\frac{(1+\left(\frac{f}{f_1}\right)^2}{(1+\left(\frac{f}{f_2}\right)^2}} \tag{11}$$

The coefficient of surface reflection can be calculated using the Bechmann-Spezzichino model [18] as proposed in [19] so the magnitude value of the reflected surface coefficient can be formulated as in (11). In the formula, $f_2 = 378/w^2$ and $f_1 = 10^{0,5} f_2$.. The unit of f is in kHz and w represents the wind speed in knots [20]. If there is a phase shift of π due to the reflection of the sea surface, so the surface reflection coefficient of the complex becomes:

$$\tilde{r}_s = -\left|\tilde{r}_s\right| \tag{12}$$

The bottom reflection coefficient was estimated using Rayleigh modeling [21] and NUSC modeling [22]. Meanwhile, the pressure losses caused by reflections of the repetitive surface and the sea bottom for each multipath can be expressed as in the following equations:

$$R_{SS_x} = \tilde{r}_s^{\,x}\, \tilde{r}_b^{\,x-1} \cong -\left|\tilde{r}_s\right|^x$$

$$R_{SB_x} = \tilde{r}_s^{\,x}\, \tilde{r}_b^{\,x} \cong \left|\tilde{r}_s\right|^x$$

$$R_{BS_x} = \tilde{r}_s^{\,x}\, \tilde{r}_b^{\,x} \cong \left|\tilde{r}_s\right|^x$$

$$R_{BB_x} = \tilde{r}_s^{\,x-1}\, \tilde{r}_b^{\,x} \cong -\left|\tilde{r}_s\right|^{x-1} \tag{13}$$

where x = 1,2,…,∞. The amplitudes of each of the four types of multipath signals can be calculated as the following equations:

$$\alpha_{SS_x} = \frac{D}{SS_x} R_{SS_x}$$

$$\alpha_{SB_x} = \frac{D}{SB_x} R_{SB_x}$$

$$\alpha_{BS_x} = \frac{D}{BS_x} R_{BS_x}$$

$$\alpha_{BB_x} = \frac{D}{BB_x} R_{BB_x} \tag{14}$$

C. System Model

In this simulation, PTR communication is used as a method of signal transmission on UAC.

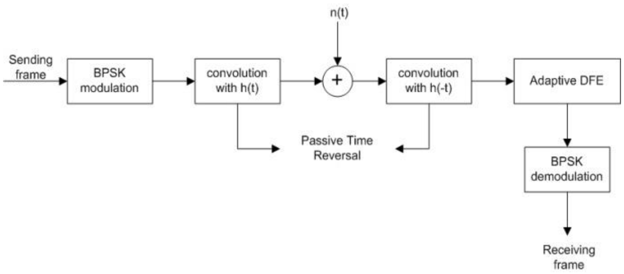

Fig. 2. Passive-time reversal communication scheme

PTR is easier to implement compared to ATR and it does not require additional time between receiving signals and transmitting signals back to the source. As an implementation of the PTR communication process, the simulation begins with the generation of the transmitted signal. The transmitted signals are modulated first with the BPSK modulation scheme, and they pass through the multipath channel that has been modeled by geometry-based modeling, and then the transmitted signal is convoluted with the channel impulse response. At the receiver, TR process is carried out and then the equalizer receives the time-reversed signal as an input.

The quantizer of DFE replaces every positive value of the input signal to the detector with „+1" and every negative value with „-1". A very simple form of quantizer could be a sign function. The improved LMS algorithm is used to minimize the mean square error (MSE) formed from the subtraction of output and input of the quantizer. Assuming that the detector has so far made correct decisions, the input to the FB filter is the previously transmitted symbols provided by the detector. To simplify the communication model, the complex environmental noise is assumed to be Additive White Gaussian Noise (AWGN). Fig. 2 shows the model system for simulation.

The geometry-based channel model refers to the real towing tank conditions that have dimensions of 200 m length, 12 m width, and 6 m depth and the pool walls are made of concrete as shown in Fig. 3. The model utilizes the impulse response of the channel by weighting according to the attenuation due to reflection or absorption that occurs. The bottom condition of towing tank is flat and the medium is fresh water, no waves, and no transient noise in the environment around the towing tank.

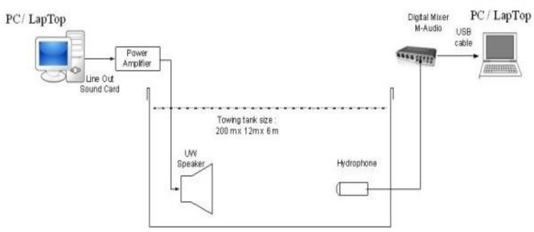

Fig. 3. The measurement scenario on towing tank

III. RELATED WORKS: JOINT PASSIVE TIME REVERSAL AND ADAPTIVE DFE

In the communication process, the information signal consists of a series of symbols that are notated I_m and each symbol has a duration of T, then the baseband data signal can be expressed as follows:

$$s(t)=\sum_{m} I[m] g(t-mT) \tag{15}$$

where *g (t)* is a pulse shape function for each symbol, so that:

$$g(\tau)=\begin{cases}1, & for\, 0\le\tau<T\\ 0, & otherwise\end{cases} \tag{16}$$

Signals received on the k^{th} receiver in the UAC can be expressed by the following equation:

$$r_k(t)=h_k(t)*s(t)+w_k(t) \tag{17}$$

In equation (17), h_k is the impulse response channel, w_k is a band-limited noise, while the notation * shows the convolution of the transmitter filter and the receiver filter with the impulse response function. The impulse response of the UAC between the transmitter and the receiver can be expressed as follows:

$$h_k(t)=\sum_{i=1}^{J}\alpha_i\delta(t-\tau_i) \tag{18}$$

where α_i and τ_i are the amplitude of each multipath (tap coefficient) and the time delay of i^{th} path respectively. Then the received signal r_k (t) is demodulated to be a baseband signal $v_k(t)$ at the k^{th} receiver.

$$v_k(t)=\sum_{m} I[m] h_k(t-mT) e^{j\theta_k(t)}+w_k(t) \tag{19}$$

where $\theta_k(t)$ denotes a frequency shift caused by a Doppler shift. In equation (17), the match-filtering process on the received signal is applied, and the output produced after the match-filtering process can be expressed as follows:

$$z(t)=\sum_{k=1}^{M} h_k(-t)*v_k(t)$$

$$=\sum_{k=1}^{M} h_k(-t)*\sum_{m} I[m] h_k(t-mT)e^{j\theta_k(t)}+\sum_{k=1}^{M} h_k(-t)*w_k(t)$$

$$=\sum_{m} I[m]\sum_{k=1}^{M} h_k(-t)*h_k(t-mT)e^{j\theta_k(t)}+\zeta_k$$

$$=\sum_{m} I[m]\sum_{k=1}^{M} Q_k(t-mT)e^{j\bar{\theta}_k(t)}+\zeta_k \tag{20}$$

Q_k (t) denotes the autocorrelation of the impulse response function h_k (t), $\bar{\theta}_k$ is the carrier frequency shift after M-channel combining, while ζ_k (t) is filtered noise. The performance of the passive reversal time depends on the function of $Q_k(t)$. If $Q_k(t)$ does not approach the Dirac function, then the side lobes of Q_k (t) may cause ISI. The ISI can be reduced by time reversal refocusing. It is assumed that there are M receivers and they are using equal weight combining.

As a nonlinear equalizer DFE has a common form as follows:

$$\hat{I}_k^{\,n}=\sum_{j=-N_{ff}+1}^{0} a_k^j V_k^{n-j}+\sum_{j=1}^{Nfb} b_k^j\tilde{I}_k^{\,n-j} \tag{21}$$

where a = $\{a_k^0,\dots,a_k^{Nff-1}\}^*$ and b_k = $\{b_k^1,\dots,b_k^{Nfb}\}^*$ are tap coefficient vectors for feed forward and feedback filters with each length of N_{ff} and N_{fb}. $\tilde{I}_k^{n-j}$ denotes the symbol of the best decision result that approximates the estimated symbol $\hat{I}_k^{n-j}$. Fig. 4 shows the block diagram of DFE. When compared to the linear equalizer, in the DFE there is a feedback loop where filter B_k (z) uses $\hat{I}_k^n$ as input, so DFE becomes non-linear. W_n^k denotes the additive noise, A_k (z) and B_k (z) denotes the z transforms of tap, a_k and b_k coefficients for forward feed filters and feedback respectively, where $z = e^{j\omega t}$. The b_k value is uniquely determined by the CIR. Although N_{ff} is independent of CIR, a_k and b_k are interrelated. Assuming that the previous symbol is correctly detected in the feedback filter, the tap coefficient is obtained by minimizing the MSE output. Block diagram of the TR receiver combined with adaptive DFE is shown in Fig. 5. The LMS algorithm is used to update the tap weights. The baseband signal is converted to N samples per symbol for digital signal processing. When estimating the n^{th} symbol, then the k^{th} channel feedforward filter tap weight vector can be formulated as follows:

$$a_k'[n] = \left\{a_1^k[n], \ldots, a_{Nff}^k[n]\right\}^* \tag{22}$$

For down-sampling at a random initial instant, two samples per symbol DFE is sufficient to correct synchronization errors for the signal, which has a bandwidth of 1/T. The input samples to the feedforward filter of the N_{ff} taps are written as a vector :

$$v_k[n] = \left\{v_k[nT], v_k\left[nT - \frac{T}{2}\right], \ldots, v_k\left[n - \frac{N_{ff}T}{2}\right]\right\}^T \tag{23}$$

The tap coefficient vector for the feedback filter is written as:

$$b_k'[n] = \left\{b_1^k[n], \ldots, b_{Nfb}^k[n]\right\}^* \tag{24}$$

where N_{fb} is the number of feedback taps, and the vector is updated at the symbol rate 1/T.

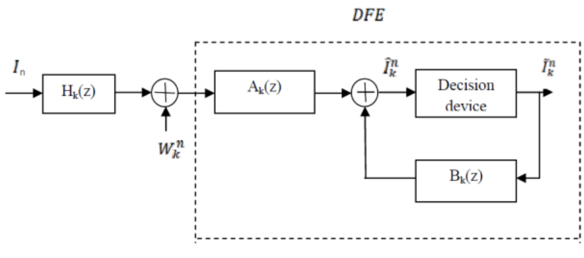

Fig. 4. Block diagram of adaptive DFE

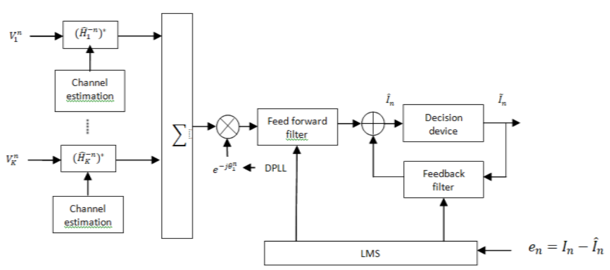

Fig. 5. Block diagram of joint PTR and ADFE

The feedback filter's input vector is:

$$d[n] = \left\{\hat{I}[n-1], \ldots, \hat{I}[n - N_{fb}]\right\} \tag{25}$$

where $\hat{I}[n]$ is the decided output, which is the closest symbol to the estimated symbol $\tilde{I}[n]$. The combining of the M-channel estimates is used to get $\tilde{I}[n]$.

$$\tilde{I}[n] = \left\{a_1'[n], \ldots, a_K'[n], -b'[n]\right\} \begin{Bmatrix} v_1[n]e^{-j\hat{\theta}_1} \\ \vdots \\ v_K[n]e^{-j\hat{\theta}_K} \\ d[n] \end{Bmatrix} \tag{26}$$

$\hat{\theta}_k$ corrects the phase offset of the current symbol, and the error estimation is obtained from:

$$e[n] = I[n] - \tilde{I}[n] \tag{27}$$

where I[n] is the training symbol in the training mode. $\tilde{I}[n]$ replaces I[n] in iterations of tracking mode. The coefficient of K feed forward filters is updated by the LMS algorithm. The updated equation for the feed forward filter is:

$$a_k'[n+1] = a_k'[n] + \mu v_k[n]e[n] \tag{28}$$

The updated equation for the feedback filter is:

$$b_k'[n+1] = b_k'[n] + \mu\tilde{I}[n]e[n] \tag{29}$$

where μ is the step size which controls the size of the correction that is applied to the tap-weight vector as it proceeds from one iteration cycle to the next. The coefficients of the feedforward and feedback filter are updated by minimizing the cost. The cost function is used to minimize the MSE.

$$J_{MSE}[n] = E\left\{\left|e[n]\right|^2\right\} = E\left\{\left|I[n] - \tilde{I}[n]\right|^2\right\} \tag{30}$$

where $|e[n]|$ denotes the absolute value of e[n].

By using a sequence of training symbol and certain step size value, then the convergence of TR-DFE can be achieved. However, the characteristic of the LMS algorithm is a slower rate of convergence, hence it required a modification to its step size. In this paper, the modification of step size in the LMS is done by multiplication with the absolute value from the difference of the last two errors. Thus, the formula of the modified step-size value can be represented as in the following equation:

$$\mu(n) = \mu\left|e(n) - e(n-1)\right| \tag{31}$$

where μ is the existing step-size value, while e(n) is the last error or error at the n^{th} iteration and e(n-1) is the error value at $(n-1)^{th}$ iteration.

IV. Simulation Result and Discussion

A. Shallow Water Channel Model

The geometry-based channel model used in this paper refers to Fig. 1. The source's (transmitter) height calculated from the bottom of the pool is 3 m, and the receiver's height is 4 m. The wind speed in the room is assumed to be relatively quiet at 10 knots so that at a distance of 100 meters, the amplitude of each multipath can be obtained by using the formula in (14). Fig. 6 and 7 show the amplitude of each multipath and channel impulse response respectively.

TABLE I: A Parameter Value of Direct Signal and Multipath

Path	Type	Parameter			
		Path length (m)	Delay (second)	Amplitude (αi)	Arriving Angle
i=1	D	100,005	0	1	-0,01
i=2	SS1	100,125	8,03e-05	-0,33	0,014
i=3	SS2	101,445	9,6e-04	-0,1	0,17
i=4	SS3	104,205	2,8e-03	-0,035	0,28
i=5	SS4	108,405	5,6e-03	-0,01	0,39
i=6	SS5	114,045	9,4e-03	-0,003	0,49
i=7	SB1	100,845	5,6e-04	0,33	-0,13
i=8	SB2	103,125	2,09e-03	0,1	-0,25
i=9	SB3	106,845	4,6e-03	0,034	-0,35
i=10	SB4	112,005	8e-03	0,01	-0,46
i=11	SB5	118,605	1,24e-02	0,0033	-0,55
i=12	BS1	100,605	4e-04	0,33	0,1
i=13	BS2	102,645	1,77e-03	0,1	0,23
i=14	BS3	106,125	4e-03	0,034	0,34
i=15	BS4	111,045	7e-03	0,01	0,44
i=16	BS5	117,405	1,16e-02	0,0033	0,53
i=17	BB1	100,245	1,6e-04	-0,98	-0,07
i=18	BB2	101,805	1,2e-03	-0,32	-0,19
i=19	BB3	104,805	3,2e-03	-0,1	-0,3
i=20	BB4	109,245	6,18e-02	-0,03	-0,4
i=21	BB5	115,125	1,01e-02	-0,01	-0,5

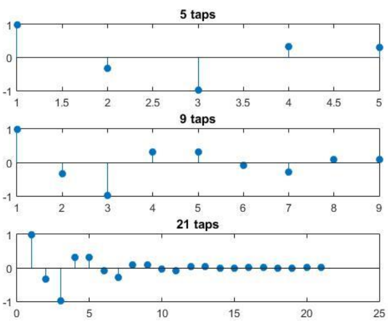

Fig. 6. The amplitude of each multipath

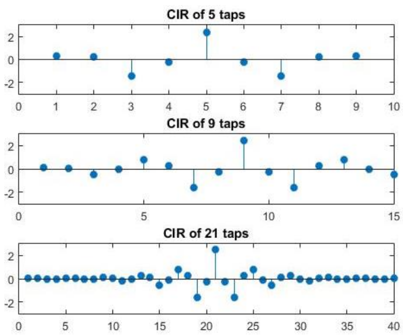

Fig. 7. The channel impulse response of each number multipath

In Table I, it can be seen that the path length of SS and BB are smaller than SB or BS. This result has an impact on the arrival time of the signal in the receiving element (τ) so the arrival time of the BB and SS path is smaller than SB and BS.

The amplitude of the channel impulse response is influenced by the attenuation (R_{ss}) value of each path. The order of each path (x) also affects the attenuation value. The amplitude of the channel impulse response decreases with increasing order value (x).

B. Analysis Performance of Joint PTR and ADFE

To improve the system performance, the receiver of TR needs to be combined with modified ADFE. In this simulation, the LMS algorithm is used to update the tap coefficient of the DFE filter. Each transmitted frame consists of 5000 training symbols, 1000000 data symbols, and a step size of 0.045 then the convergence of TR-ADFE can be achieved. Fig. 8 proves that the joint PTR and modified ADFE result in a faster convergence than PTR with the existing ADFE.

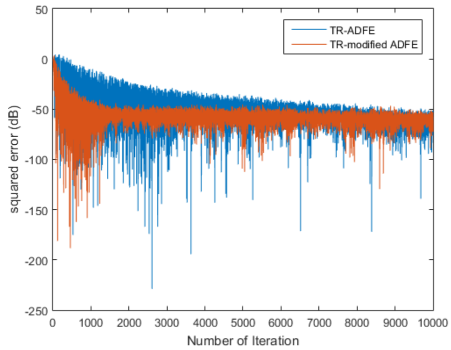

Fig. 8. The squared error of the PTR-modified ADFE and the existing PTR-ADFE

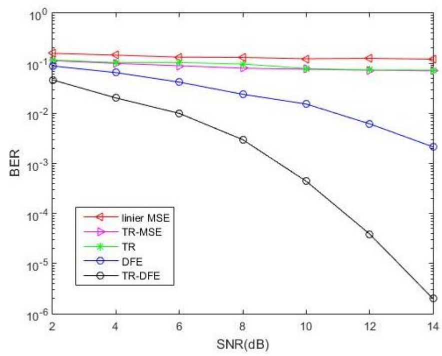

Fig. 9. Performance comparison of PTR-ADFE and other algorithms

For convenience, the convergence rate in Fig. 8 is represented using a squared error parameter expressed in dB. The joint PTR-ADFE reaches steady-state conditions at the 1500th iteration. The modified PTR-ADFE and the existing PTR-ADFE have different values of around 25 dB in that iteration and both curves are at the same steady-state value at 10000th iteration. This will also reduce the value of the MSE. Without the addition of the number of training symbols, the convergence can be obtained.

In Fig. 9, the simulation result shows that BER obtained on joint PTR and ADFE is superior to the other algorithms. The analysis of system performance is done by comparing between joint PTR-ADFE, linear equalization and its combination with TR. The difference in the BER value is significant between PTR-ADFE and the others.

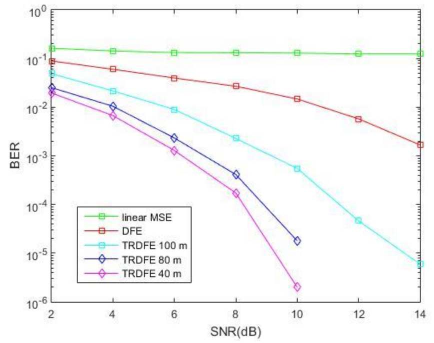

Fig. 10. Performance comparison at the various distance of source-receiver

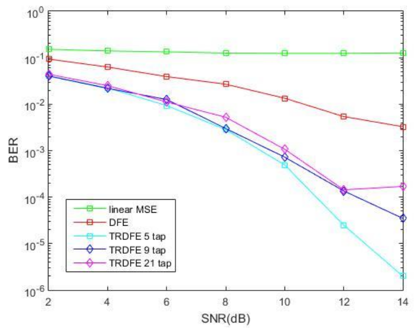

Fig. 11. Performance comparison of multipath variations

There are 6 dB differences between PTR-ADFE and DFE at the same BER value. Meanwhile, the TR combination with the linear equalization shows the worst BER value.

The observed variations in the distance between the transmitter and receiver observed starts from 40 m, 80 m, and 100 m. The simulation result in Fig. 10 shows that at 40 m the PTR-ADFE has the best result of BER value. Meanwhile, at 40 m the linear equalization and DFE shows a worse performance compared to PTR-ADFE at 80 m and 100 m. This effect due to the greater distance resulting in attenuation experienced by the signal is also getting bigger.

Multipath in shallow water environment varies according to the environmental conditions. They will affect the performance of the TR communication system in UAC. By using a geometry-based channel model the effect of multipath numbers can be observed more clearly. In this simulation, the performance of the PTR-ADFE is compared to the environment with the various number of multipath ranging from 5 taps up to 21 taps. The BER value shown in Fig. 11 proves that the best performance is obtained in the environment with 5 taps of multipath.

V. Conclusion

In this paper, the shallow water channel modeling based on geometry and environmental parameters have been done. The geometry-based channel model can be used to analyze the communication system performance simply and effectively. The simulation results show that PTR-ADFE is a powerful technique in overcoming multipath effects in the shallow water environment. The simulation results also prove that the combination of PTR-modified ADFE can minimize the error and improve the convergence rate of the existing system. BER value is obtained when the distance transmitter and receiver 40 m is close to 10^{-6} at SNR 10 dB. At a distance of 40 m, the PTR-ADFE performance has the best performance compared to the distance of 80 m and 100 m. PTR-ADFE performance in a sparse multipath environment has a superior performance to a rich multipath environment. On the underwater acoustic channel with a number of 5 tap paths, the BER value approaches 10^{-6} at the 14 dB SNR. For further research, PTR-ADFE can be implemented to take into account the Doppler effects and environmental noise. To achieve the real conditions, so the experiment can be carried out in a real environment such as a lake or shallow sea.

Acknowledgment

We would like thank to Ministry of Research, Technology and Higher Education of the Republic of Indonesia through the 2019 Doctoral Dissertation Research (PDD)

References

[1] D. B. Kilfoyle and A. B. Baggeroer, “The state of the art in underwater acoustic telemetry,” *IEEE J. Ocean. Eng*., vol. 25, pp. 4–27, 2000.

[2] D. Rouseff, M. Badiey, and A. Song, “Effect of reflected and refracted signals on coherent underwater acoustic communication: Results from the Kauai experiment (KauaiEx 2003),” *J. Acoust. Soc. Am*., vol. 126, pp. 2359–2366, 2009.

[3] A. Song, M. Badiey, H. C. Song, S. Hodgkiss, and M. B. Porter, “Impact of ocean variability on coherent underwater acoustic communications during the Kauai experiment (KauaiEx),” *J. Acoust. Soc. Am.*, 123, pp. 856–865, 2008.

[4] D. Rouseff, D. Jackson, W. Fox, C. Jones, J. Ritcey, and D. Dowling, “Underwater acoustic communications by passive-phase conjugation: Theory and experimental results,” *IEEE J. Ocean. Eng.,* vol. 26, pp. 821-831, Oct. 2001.

[5] D. F. Yarger, “The user guide for the RAY-MODE propagation loss program,” *NUSC Technical Memorandum*, Aug. 1976.

[6] G. Edelmann, H. Song, S. Kim, W. Hodgkiss, W. Kuperman, and T. Akal, "Underwater acoustic communications using time reversal," *IEEE J. Ocean. Eng*., vol. 30, pp. 852-864, Oct. 2005.

[7] G. Edelmann, T. Akal, W. Hodgkiss, S. Kim, W. Kuperman, H. Song, and T. Akal, "An initial demonstration of underwater acoustic communications using time reversal mirror," *IEEE J. Ocean. Eng*., vol. 27, pp. 602-609, Jul. 2002.

[8] T. Shimura, Y. Watanabe, H. Ochi, and H. Song, "Long-range time reversal communication in deep water: Experimental results," *J. Acoust. Soc. Am.*, vol. 132, EL49–EL53, 2012.

[9] H. Song, W. Hodgkiss, W. Kuperman, M. Stevenson, and T. Akal, "Improvement of time reversal communications using adaptive channel equalizers," *IEEE J. Ocean. Eng.*, vol. 31, pp. 487-496, Apr. 2006.

[10] H. Song, W. Hodgkiss, W. Kuperman, W. Higley, K. Raghukumar, and T. Akal, "Spatial diversity in passive time reversal communications," *J. Acoust. Soc. Am.*, vol. 120, pp. 2067-2076, Oct. 2006.

[11] G. S. Zhang and H. F. Dong, "Joint passive-phase conjugation with adaptive multichannel combining for coherent underwater acoustic communications," *J. Applied Acoustics*, vol. 73, pp. 433-439, Apr. 2012.

[12] M. Stojanovic and L. Freitag, "Acquisition of direct sequence spread spectrum acoustic communication signals," in *Proc. 2003 Oceans*, Sep. 2003, vol. 1, pp. 22-26.

[13] G. S. Zhang and H. F. Dong, "Spatial diversity in multichannel processing for underwater acoustic communications," *J. Ocean Engineering*, vol. 38, pp. 1611-1623, Oct. 2011.

[14] M. Stojanovic, J. A. Capitovic, and J. G. Proakis, "Adaptive multichannel combining and equalization for underwater acoustic communications," *J. Acoust. Soc. Am.*, vol. 94, pp. 1621–1631, 1993.

[15] T. C. Yang, "Differences between passive-phase conjugation and decision-feedback equalizer for underwater acoustic communications," *IEEE J. Ocean. Eng.*, vol. 29, no. 2, pp. 472–487, Apr. 2004.

[16] T. C. Yang, "Correlation-based decision-feedback equalizer for underwater acoustic communications," *IEEE J. Ocean. Eng.*, vol. 30, no. 4, pp. 865–880, Oct. 2005.

[17] H. Song, "An overview of underwater time-reversal communication," *IEEE J. Ocean. Eng*., vol. 41, pp. 644–655, 2016.

[18] B. Li, H. Yang, G. Liu, and X. Peng, "A new joint channel equalization and estimation algorithm for underwater acoustic channel," *J Wireless Com Network*, 2017.

[19] R. Diamond, *Extend Users Manual*, San Jose, CA: Imagine That, Inc., 1988.

[20] R. Coates, "An empirical formula for computing the beckmann-spizzichino surface reflection loss coefficient," *IEEE Trans. Ultrason. Ferroelec. Frequency Contr.*, vol. 35, no. 4, pp. 522-523, July 1988.

[21] P. Wang, L. Zhang, *et al*., "A stratified acoustic model accounting for phase shifts for underwater acoustic networks", *Sensors(Basel)*., vol. 13, no. 5, pp. 6183-203. May 2013.

[22] L. M. Brekhovskikh, *Waves in Layered Media*, 2nd ed. New York: Academic Press, 1980, pp. 299-305.

Yuning Widiarti received her B.E. degree in Telecommunication Engineering and M.E. degree in Control System from Institut Teknologi Sepuluh Nopember (ITS) in 2005 and 2011 respectively. She is currently a Ph.D. candidate in Telecommunication Multimedia at Institut Teknologi Sepuluh Nopember (ITS). Her research interests are in the areas of time reversal communication in underwater acoustic channel.

Wirawan received his B.E. degree in Telecommunication Engineering from Institut Teknologi Sepuluh Nopember (ITS) in 1982, and completed his Master of Engineering from Ecole Supérieure en Sciences Informatique – Univ. de Nice Sophia Antipolis in 1996 and the Ph.D degree in signal and image processing from Télécom ParisTech (d/h Ecole Nationale Supérieure des Télécommunication) in 2003. He joined the Department of Electrical Engineering, ITS as a Lecturer in 1989. His research interests include multimedia communication, signal processing, wireless sensor network, and underwater acoustics.

Suwadi received his B.E. degree in Telecommunication Engineering from Institut Teknologi Sepuluh Nopember (ITS) in 1992, M.E. degree in Electrical Engineering from Institut Teknologi Bandung (ITB) in 1999, and Ph.D. degree in Telecommunication Multimedia at Institut Teknologi Sepuluh Nopember (ITS) in 2012. He joined the Department of Electrical Engineering, ITS as a Lecturer in 1993. His research interests include digital communication system, wireless network, digital signal processing, and antenna and propagation system.